Neutron Imaging Camera

S. D. Hunter*[a], G.A. de Nolfo[b], L.M. Barbier[a], J.T. Link[c], S. Son[b],
S.R. Floyd[a], N. Guardala[d], M. Skopec[d], B. Stark[d]
[a]NASA/Goddard Space Flight Center, Code 661, Greenbelt, MD, USA 20771;
[b]UMBC/CRESST/NASA, Code 661, Greenbelt, MD USA 20771;
[c]USRA/CRESST/NASA, Code 661, Greenbelt, MD USA 20771;
[d]Naval Surface Warfare Center, Carderock, MD USA 20814

ABSTRACT

The Neutron Imaging Camera (NIC) is based on the Three-dimensional Track Imager (3_DTI) technology developed at GSFC for gamma-ray astrophysics applications. The 3-DTI, a large volume time-projection chamber, provides accurate, ~0.4 mm resolution, 3-D tracking of charged particles. The incident direction of fast neutrons, En > 0.5 MeV, are reconstructed from the momenta and energies of the proton and triton fragments resulting from $^{3}He(n,p)^{3}H$ interactions in the 3-DTI volume. The performance of the NIC from laboratory and accelerator tests is presented.

Keywords: Micro-well detector (MWD), Neutron Imaging Camera (NIC), WGPu, HEU

1. INTRODUCTION

The Department of Defense has been tasked to develop a means of standoff passive interrogation to detect small quantities of WGPu and moderate amounts of HEU via both passive and active interrogation. WGPu typically contains 6-10% ^{240}Pu which emits a continuous spectrum of neutrons with a broad unshielded (unmodulated) peak with energies between ~0.2 and ~5 MeV. Shielding of this material decreases, but does not eliminate, the flux of these energetic (fast) neutrons. The fast neutrons that penetrate through the shielding are minimally scattered traversing the atmosphere and retain their directional information. A detector capable of imaging these fast neutrons is able to quickly, and with very low probability of false detection, determine the location of WGPu at a standoff distance and in the presence of background emission. HEU and some newer Pu devices without ^{240}Pu, may require a high-dose neutron field for interrogation, resulting in a specific neutron response from the device but in a high-field background.

The Neutron Imaging Camera (NIC) is based on NASA/GSFC's Three-Dimensional Track Imager (3-DTI) detector technology being developed for medium- and high-energy gamma-ray telescopes. The 3-DTI, a large volume time-projection chamber (TPC) with two-dimensional micro-well readout (MWD), provides accurate, ~0.4 mm resolution, 3-D tracking of charged particles. The incident direction of fast neutrons, E_n > 0.5 MeV, are reconstructed from the momenta and energies of the proton and triton fragments resulting from $^{3}He(n,p)^{3}H$ interactions in the 3-DTI volume.

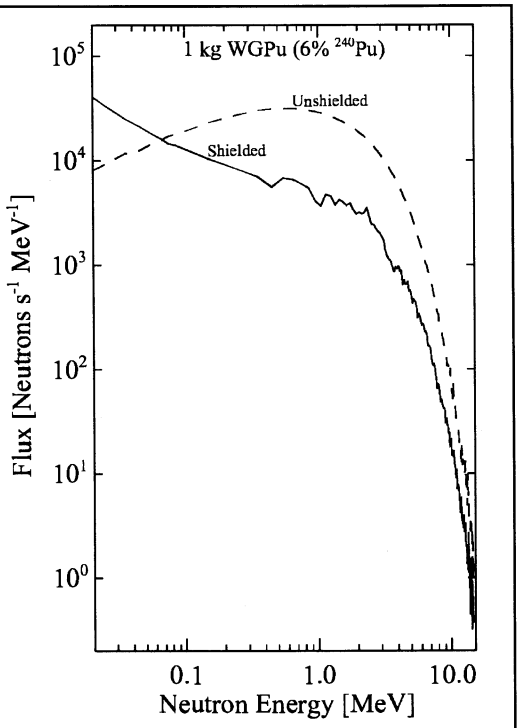

Fig. 1. Intensity of neutrons from SNM with and without shielding (shielding: 10 cm spherical shell of water surrounding 5 cm spherical shell of iron surrounding the

1.1 Objective

We describe the development of a 10 × 10 × 15 cm^3 NIC prototype detector, Figure 2, and subsequent tests in the laboratory using ^{242}Cf and AmBe sources. The goal of the NIC design is to provide a large cubic meter, high-resolution camera, with full 360° azimuth sensitivity, that is capable of passively detecting WGPu and HEU at reasonable stand-off distances. For neutrons with energies > 0.5 MeV, there is virtually no naturally occurring background. Figure 2 shows a simulation based on MCNPX of both shielded and unshielded neutron flux from WGPu. For fast neutrons with energies above 0.5 MeV, the intensity is reduced but still measurable. In addition, neutrons suffer minimal scattering in the atmosphere and thus still retain directional information.

We plan to develop a NIC camera that is sensitive to 1 kg of WGPu at a stand-off distance of 100 m with an integration time of 30 s and also sensitive to 8 kg of HEU at 10 m stand-off distance over 25 minutes integration time. In addition, the NIC camera can operate in an active interrogation mode with the use of a commercially available D-T neutron generator, producing 10^6 N/s/cm^2. With neutron interrogation, we envision a NIC camera that can actively detect 8 kg of HEU at 100 m in 30 s^2. To reach these design goals requires a NIC camera that is 1 m^3 and is sensitive in 360° azimuth. The development of NIC will take place in three stages, starting with the already built and tested 10×10×15 cm^3 prototype, followed by a scale up 50×50×30 cm^3 prototype, and finally a 1 m^3 NIC camera that will be ready for realistic platforms.

Goal	Desirable	Minimal
WGPu, passive detection	1 kg at 100 m in 30 s	1 kg at 100 m in 10 min
HEU, passive detection	8 kg at 10 m in 25 min	8 kg at 10 m in 60 min
HEU, active detection [1]	8 kg at 100 m in 30 s [2]	8 kg at 100 m in 10 min

\

2. TECHNICAL DESCRIPTION

The Neutron Imaging Camera (NIC) is designed to image fast neutron sources, En > 0.5 MeV. The underlying principle is to measure the energy and position in three dimensions of charged particles traversing the camera medium. Neutrons entering the camera are identified by the detection of the interaction products, a proton and a triton, from the reaction $^3He(n,p)^3H$. The incident direction of fast neutrons is reconstructed on a neutron-by-neutron basis from the measure of the proton and triton energy and momenta.

NIC is comprised of a large volume gas time projection chamber (TPC) with two-dimensional, gas micro-well detector (MWD) readout, see Fig. 2. The TPC is filled with a ^3He gas mixture that acts as a large volume, low density, homogenous tracker. Incident neutrons enter the TPC and undergo inelastic and elastic scatters. In the case of inelastic scatters, the reaction products, the proton and triton, travel through the chamber leaving an ionization trail along their trajectory. The TPC measures the position of the charge particle track and the energy loss by ionization in the gas. It is bounded at the top with a drift electrode and an array of MWDs at the bottom. A cage of field shaping wires defines the sides of the active volume and provides a uniform drift field (~200V/cm). The ionization charge along the tracks drifts toward the MWDs at the bottom. The MWDs are a two-dimensional array of gas proportional counters. The MWDs are orthogonal electrode strips rigidly affixed to an insulating substrate. The wells themselves are defined by holes in the cathode strips and in the insulators that expose the orthogonal anode strips below. The micro-wells are maintained at a bias voltage that establishes an intense electric field 10^4-10^5 V/cm, so that the charge, as it enters the wells, undergoes an ionization avalanche. The electrons are collected on the anode while equal and opposite charges are set up on the cathodes. The orthogonal strips, thus, provide 2D imaging.

---

[1] Using a modest, commercially available, hand carried D-T neutron generator capable of producing 10^6 N/s/cm^2. Higher flux neutron sources would increase the detection distance and/or reduce the interrogation time.

[2] Shielding effects of the neutrons, both incoming, and outgoing are taken into account.

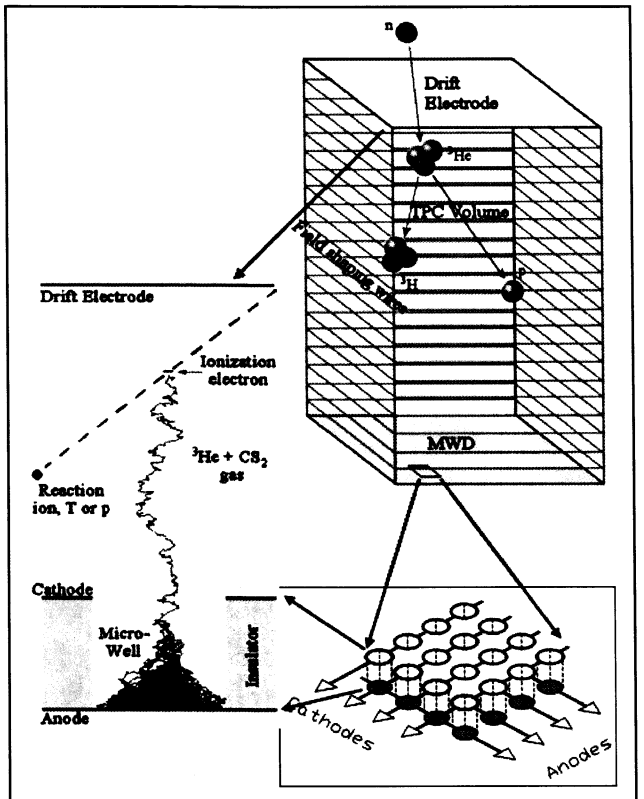

Fig. 2 : Schematic diagram of the Three-Dimensional Track Imager (3-DTI), time projection chamber (TPC) volume, two-dimensional micro-well detector (MWD), and micro-well operation. The TPC drift field is defined by the cathode plane and the drift electrode. An energetic charged particle traversing the TPC produces ionization electrons that drift into the micro-wells, where, in the intense electric field, they

To achieve 3-D reconstruction of a track, the *z*-coordinate of the ionization charge is determined by recording the time structure of the avalanche charge signals on each anode and cathode. The drift velocity of the ionization charge in the gas determines the translation from time to spatial coordinate. The drift velocity of the ionization charge (free electrons) in He is on the order of XX mm/μs, but depends strongly on additive gases (CH_4, CO_2, CH_3NO_2, etc.) and drift field (Piesart & Sauli, 1984). Furthermore, because this velocity is significantly higher than the thermal velocity of the gas, electron drift has significant longitudinal and transverse diffusion that smears out the spatial structure of the ionization charge (track structure) after only a few cm of drift. The drift velocity of the ionization charge can be substantially reduced by the addition of gaseous CS_2, a molecule with moderate electron affinity that efficiently scavenges the ionization electrons forming negative anions. The anions drift in thermal equilibrium with the gas and their drift velocity, ~0.003 mm/μs, is about 10^{-3} of that for free electrons (Martoff et al. 2004). Drifting in thermal equilibrium also substantially reduces the transverse and longitudinal diffusion (Martoff et al. 2000), greatly increasing the maximum drift distance. These anions drift towards the anodes where, in the strong electric field of the microwell, the electrons are stripped off and an electron cascade is produced in the well. In addition, the slow drift velocity reduces the required sampling rate of the transient digitizers that record the arrival time of the ionization charge.

The signals from each anode and cathode are processed though front-end electronics and a transient digitizer. Each FEE consists of a charge sensitive pre-amplifier and a pulse shaper with gain. The charge avalanche in a well induces the same and opposite polarity signal and both signals are readout through an anode and a cathode, respectively. The Transient Digitizer (TD) consists of a differential receiver, 12-bit ADC, and a common control FPGA. The TD operates at a sampling rate of 2.5Msamples-s^{-1} (i.e., the FEE is read out every 400 ns). After the analogue signal is digitized, the value is stored in a circular buffer with a size of 32,000 Samples/channel. Events, satisfying a trigger threshold, are captured by a PC via USB interface.

3. MANUFACTURE AND PERFORMANCE CHARACTERISTICS

3.1 MWD Manufacturing and Performance

We previously developed an in-house UV laser ablation technique for fabrication of 5×5cm^2 MWDs (Deines-Jones 2002b) and demonstrated stable proportional operation at gas gains up to 3×10^4, spatial resolution of ~200 μm (Black et al. 2000, Deines-Jones et al. 2002a), and FWHM energy resolution of 10% at 20 keV in P-10 (90% Ar / 10% CH_4) and 18% resolution at 6 keV in 95% Xe/5% CO_2. We are currently setting up our laboratory for the development of in-house MWDs in order to fine-tune the fabrication process.

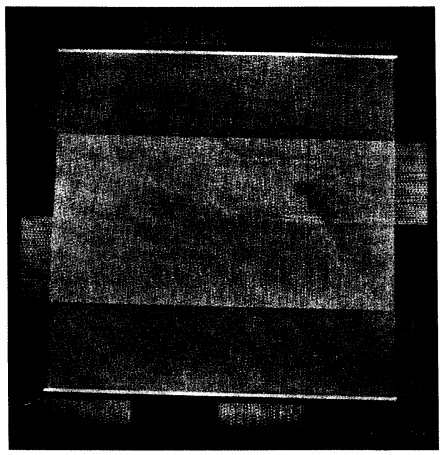

Fig. 3. Micro-well detector.

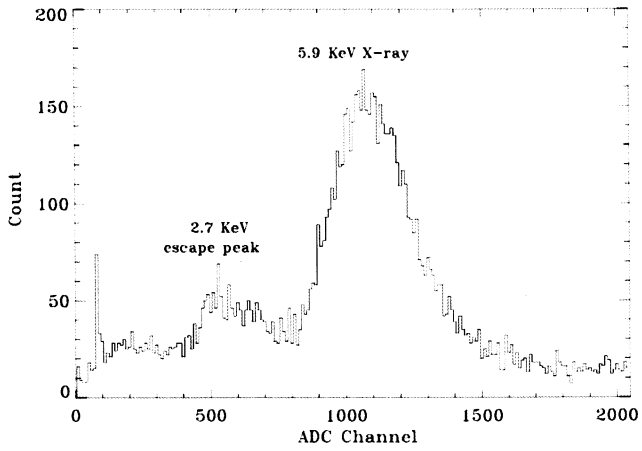

Fig. 4. Energy Spectrum from ^{55}Fe obtained from a portion of NIC. The 6 keV and argon escape peak (~3keV) are readily visible.

We have been working with several commercial vendors to develop viable fabrication processes that can be scaled to 50×50 cm^2 areas (Hunter, 2006). MWDs with 10×10 cm^2 areas have been produced and tested, see Figure 3. The micro-wells are 200 μm in diameter and 200 μm deep, on 400 μm x 400 μm center-to-center pitch. We have integrated these MWDs into a 10×10×15 cm^3 NIC prototype. We demonstrate an energy resolution of ~18% using an ^{55}Fe source in the lab with P-10/CS_2. Figure 4 shows the ^{55}Fe spectrum obtained with the 5.9 keV x-ray peak and the argon escape peak at ~3 keV.

3.2 NIC Prototype Performance

Figure 5 shows our 10×10×15 cm^3 prototype NIC in the laboratory without the vacuum chamber. The field-shaping grid rests on top of the MWD. The active volume of the TPC is bounded by this field-shaping grid. The entire camera is encased within a pressure chamber. The MWD and grid is located above a motherboard, which acts both as a seal for the pressure chamber and connects the detector high voltage and signal cables as well as the FEE low power to the power supplies and TD outside the chamber. . The volume of this prototype is large enough to fully contain the proton and triton from the majorty of neutron interactions, making it possible to fully reconstruct their energies. This is possible since the pulse height of the signal registered in the MWD is directly proportional to the energy loss, dE/dx, along the track. Provided the tracks are fully contained, the measured energy loss along the track can be used to derive spectroscopic information about the neutron source. We tested the 10×10 cm^2 prototype in laboratory and successfully imaged neutron interactions in the laboratory using a ^{252}Cf and Am-Be sources. The TPC was filled with a gas mixture of 25% 3He, 50% 4He and 25% CS2 at a total pressure of 0.4 atm. The grid voltage was held at a bias voltage of 2500 volts, and the anode/cathode bias voltage is 660 volts.

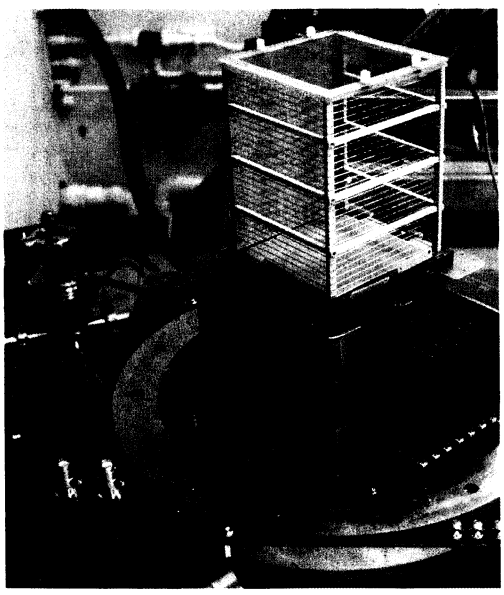

Fig. 5. NIC prototype in laboratory without vacuum chamber.

Figure 6 shows an example of an inelastic scatter of a low energy (< 0.5 MeV) neutron. The two images show the track signal in x (right) versus sample time and in y (left) versus sample time. The

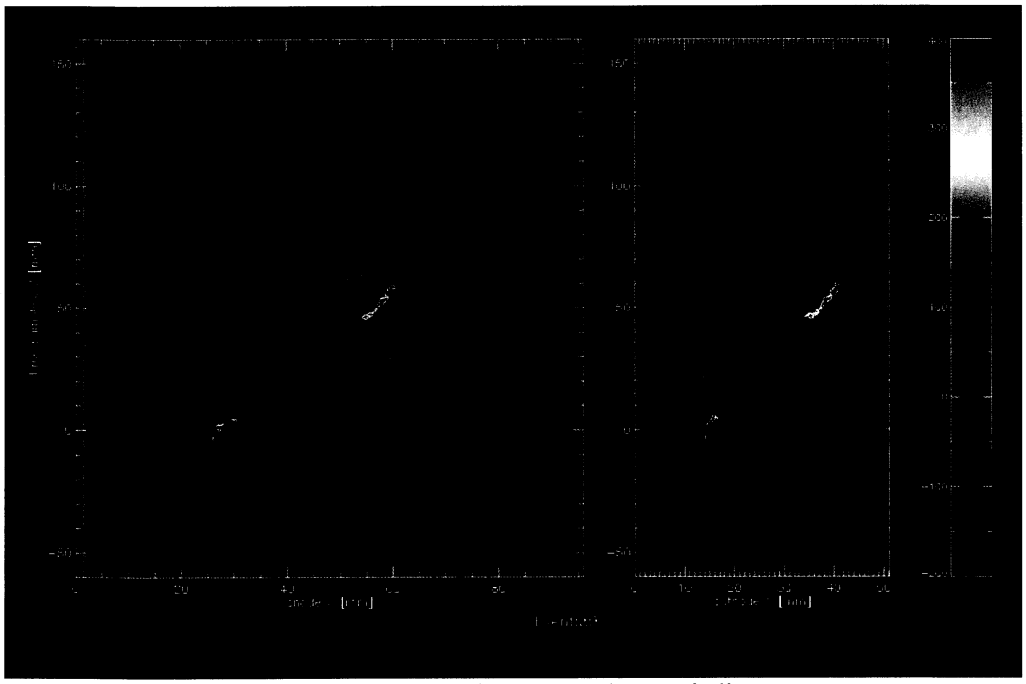

Fig. 6. Low energy neutron inelastic scatter in NIC. Red arrow indicates vertex.

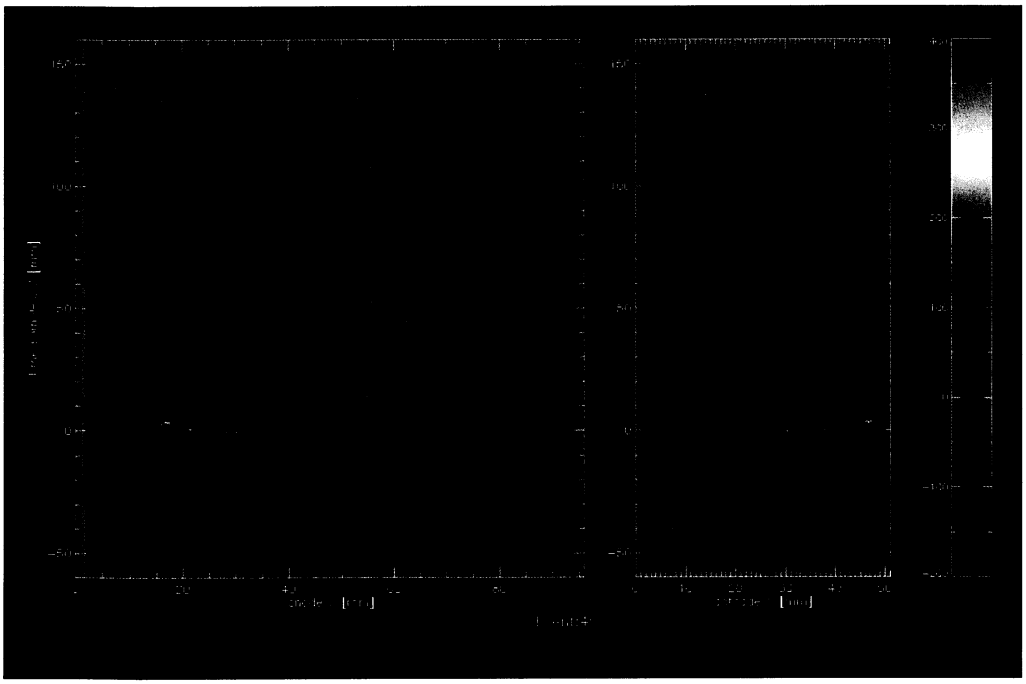

Fig. 7. Fast neutron inelastic scatter in NIC. Red arrow indicates vertex.

origin of the vertex shows the location of the scatter while the tracks represent the ionization trails of the reaction products, the proton and triton. The color scale represents the amplitude of the pulse-height along the track, which is proportional to the energy loss, d*E*/d*x*. Evident in Figure 6 is the increase in pulse height toward the end of the proton

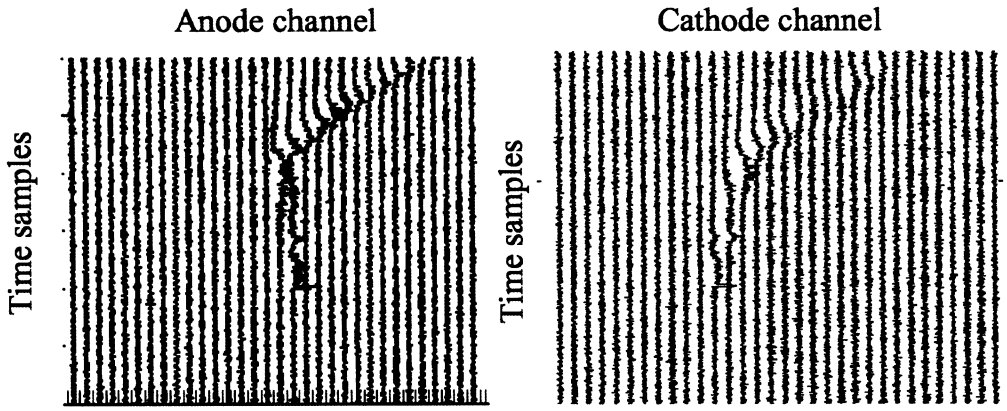

Fig. 8. Fast neutron scatter in NIC. Left: Anode signal versus time sample. Right: Cathode signal versus time sample. Red arrow indicates vertex.

and triton track, demonstrated the well-known Bragg behavior of energy loss through ionization. Figure 7 shows an example of a fast neutron interaction in NIC (1 > MeV) using an AmBe source in the laboratory.

Figure 8 illustrates the detection of a fast neutron interaction (1 > MeV). In this Figure we show the actual pulse-heights along the tracks. The temporal coincidence of the anode and cathode signals enables the raw TD signal to be translated into three spatial coordinates and energy deposition. The *x*- and *y*-coordinates of the TD signals are determined from the anode and cathode signals and the z-coordinate is determined from the sample time and the negative ion drift velocity. Figure 9 shows the reconstructed image in three dimensions of the neutron interaction. Complete reconstruction of this

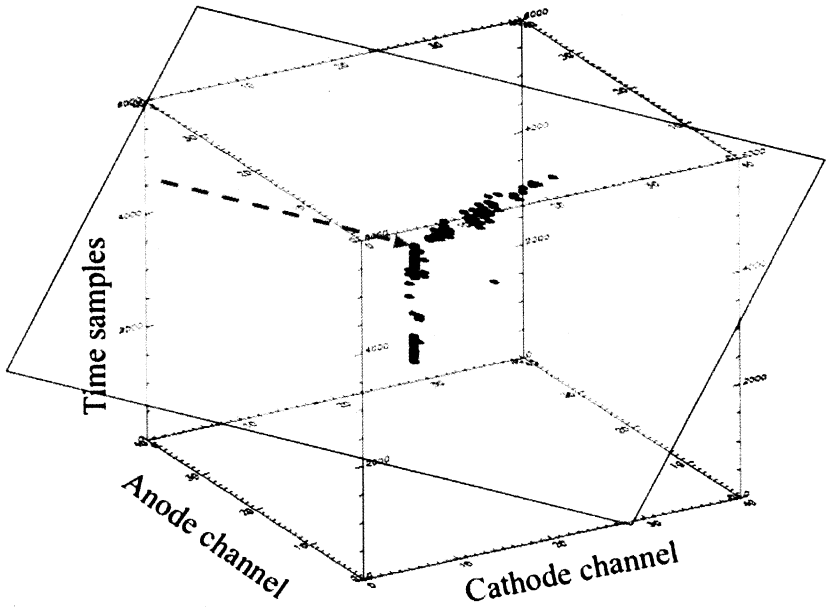

Fig. 9. Reconstruction in 3-D of fast neutron interaction in NIC. Red arrow indicates incident direction of neutron.

event was not possible, as the neutron and triton existed from the active volume. Nevertheless, the red arrow indicates our best estimate of the incident neutron direction.

4. ACCELERATOR TESTS AND SIMULATIONS

We are currently testing the response uniformity of the MWDs in the laboratory and investigating the gain characteristics of different gas mixtures for the TPC, such as He/CS_2 and He/CH_3NO_2. Complete characterization of the energy resolution and angular resolution will be obtained with an accelerator run at the Positive Ion Accelerator Facility (PIAF) at the Naval Surface Warfare Center in Carderock, MD. The tandem ion accelerator is a Pelletron design, produced by NEC, capable of accelerating positive ions with 3MV maximum acceleration voltage. The accelerator produces a monoenergetic beam of gamma rays between 0.2-15 MeV and neutrons with energies up to 8 MeV.

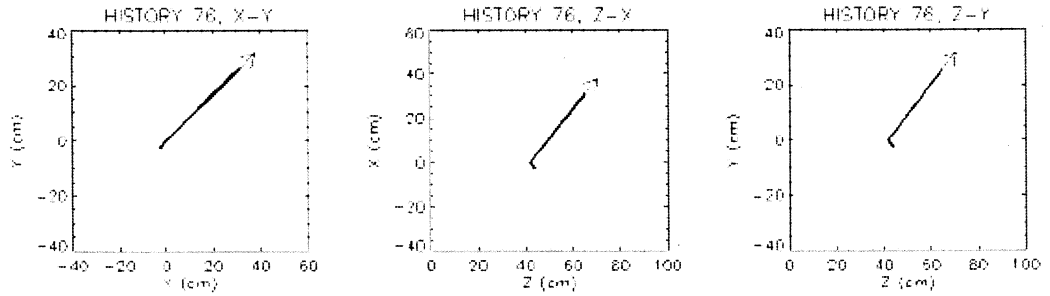

Fig. 10. Simulations based on MCNPX of 2 MeV neutron in a realist model of NIC. Shown are the particle tracks for the proton (red) and triton (blue) in the *x-y*, *z-x*, and *z-y* planes. Direction of motion indicated by green arrow.

We have begun simulations of the NIC camera using MCNPX v2.6x assuming a realistic mass model for the NIC camera. The incident neutron source is modeled as a point source over a conical volume irradiating the NIC camera. We have checked the angular dependence for $^3He(n,p)T$ reaction against available data. Figure 10 shows the particle tracks simulated for 2 MeV neutrons incident on ^3He inside NIC. $^3He(n,p)T$ is an exoergic reaction with Q-factor of 763 keV. For this particle simulation history, the resulting proton and triton energies are 2.09 MeV and 0.67 MeV, respectively. We incorporate energy loss of the proton and triton and determine the number of electrons along the path using the W-factor (energy loss per ion pair formed) of 46.3 eV. Further work requires convolving these simulation results with an appropriate NIC instrument response function. We have also begun to develop a GEANT 4 simulation to study neutron interactions within NIC.

5. SUMMARY

We have successfully demonstrated the capability of imaging fast neutrons in 3-D with our prototype NIC camera. Imaging neutrons is essential for determining the location of small quantities of WGPu at a standoff distances and in the presence of background emission as well as moderate amounts of HEU. Our upcoming accelerator tests will help to further characterize the angular and energy resolution in addition to refine our image reconstruction analysis.

REFERENCES

[1] Deines-Jones, P. et al., NIM-A, 478, 130 (2002a).
[2] Deines-Jones, P. t al., NIM-A, 477, 55 (2002b).
[3] Hunter, S.D. et al., IEEE, In Publication (2006).
[4] Martoff, S. et al., NIM-A, 555, 55-58 (2004).
[5] Martoff, S. et al., NIM-A, 440, 355 (2000).
[6] Piesart, A. & Sauli, F., CERN Technical Report, CERN-84-08 (1984).